nature geoscience

SUPPLEMENTARY INFORMATION

https://doi.org/10.1038/s41561-018-0184-7

In the format provided by the authors and unedited.

Riverine evidence for isotopic mass balance in the Earth's early sulfur cycle

Mark A. Torres[1,2*], Guillaume Paris[1,3], Jess F. Adkins[1] and Woodward W. Fischer[1]

[1]Division of Geological and Planetary Sciences, California Institute of Technology, Pasadena, CA, USA. [2]Department of Earth, Environmental, and Planetary Sciences, Rice University, Houston, TX, USA. [3]CRPG, UMR 7358 CNRS-Université de Lorraine, Vandœuvre-lès-Nancy, France. *e-mail: mt61@rice.edu

Supplementary Information for: "*Riverine evidence for isotopic mass balance in the Earth's early sulfur cycle*"

Mark A. Torres, Guillaume Paris, Jess F. Adkins, & Woodward W. Fischer

Supplementary Text
Figs. S1 to S3
Table S1 to S3
References

South Africa field site River and groundwater samples in South Africa were collected from the Neoarchean Campbellrand-Malmani platform (table S3). River water samples from this region are consistent with $\Delta^{33}S_{AC} \approx 0$ ‰ (fig. S1). Similarly, all but one of the groundwater samples also yield $\Delta^{33}S$ values within two standard deviation of zero. Like other $\Delta^{33}S$ anomalies reported in the literature (e.g., Li et al., 2016), our single groundwater sample with a $\Delta^{33}S$ anomaly (+1.8 ‰) is presumed to average a small volume of rock and thus is not representative of the bulk Archean crust. Consistent with this, river waters within the same region do not show $\Delta^{33}S$ anomalies (fig. S1). Since rainwater concentration data is unavailable for the South Africa field sites, it is not possible to more quantitatively constrain $\Delta^{33}S_{AC}$ using these samples.

Superior Craton δ^{34}S River water samples collected from the Superior Craton field site show δ^{34}S values that range from +2.7 to +11.4 ‰ (table S2). Broadly, this range is consistent with the ranges observed in local rainwaters (+2 to +9 ‰; Nriagu and Coker, 1978; Caron et al., 1986) and bedrock (-0.4 to +6 ‰; Bekker et al., 2009). However, a few samples exhibit δ^{34}S values higher than either the rain or bedrock end-members. As these high δ^{34}S samples are also enriched in Cl, the sulfur isotopic enrichment may reflect contributions from urban runoff with a high δ^{34}S. Consistent with this, the predicted proportions of urban runoff derived S are positively correlated with the measured δ^{34}S values (fig. S3). While there is some scatter in this relationships, it may be due to variable proportions of crustal and rain-derived sulfur with distinct δ^{34}S values. Alternatively, some sulfate liberated by rock weathering may be exported from the catchment as a reduced phase (e.g. organic sulfur) as a result of modern S cycling, which could cause mass-dependent S isotopic fractionation. Such loss of sulfate would cause us to overestimate the fraction of sulfate sourced from atmospheric deposition and urban runoff using Equation 5. This overestimation along with any mass-dependent fractionation would not significantly bias our estimate of $\Delta^{33}S_{AC}$, but instead only add to its uncertainty.

References

L. Li, B. A. Wing, T. H. Bui, J. M. McDermott, G. F. Slater, S. Wei, G. Lacrampe-Couloume, and B. Sherwood Lollar. Sulfur mass-independent fractionation in subsurface fracture waters indicates a long-standing sulfur cycle in Precambrian rocks. *Nature Communications*, page 13252, 2016. doi: 10.1038/ncomms13252.

J. O. Nriagu and R. D. Coker. Isotopic composition of sulfur in precipitation within the Great Lakes Basin. *Tellus A*, 2826(May):365–375, 1978. ISSN 0280-6495. doi: 10.3402/tellusa.v30i4.10356.

Francois Caron, Andre Tessier, James R. Kramer, Henry P. Schwarcz, and Charles E. Rees. Sulfur and oxygen isotopes of sulfate in precipitation and lakewater, Quebec, Canada. *Applied Geochemistry*, 1(5):601–606, 1986. ISSN 08832927. doi: 10.1016/0883-2927(86)90067-3.

Andrey Bekker, Mark E Barley, Marco L Fiorentini, Olivier J Rouxel, Douglas Rumble, and Stephen W Beresford. Atmospheric Sulfur in Archean Komatiite-Hosted Nickel Deposits. *Science*, 326(5956):1086–1089, 2009. ISSN 0036-8075. doi: 10.1126/science.1177742.

Nicole L. Cates and Stephen J. Mojzsis. Chemical and isotopic evidence for widespread Eoarchean metasedimentary enclaves in southern West Greenland. *Geochimica et Cosmochimica Acta*, 70 (16):4229–4257, 2006. ISSN 00167037. doi: 10.1016/j.gca.2006.05.014.

James Farquhar, Huiming Bao, and Mark Thiemens. Atmospheric Influence of Earth's Earliest Sulfur Cycle. *Science*, 289(5480):756–758, 8 2000. doi: 10.1126/science.289.5480.756.

James Farquhar, Marc Peters, David T. Johnston, Harald Strauss, Andrew Masterson, Uwe Wiechert, and Alan J. Kaufman. Isotopic evidence for Mesoarchaean anoxia and changing atmospheric sulphur chemistry. *Nature*, 449(7163):706–709, 2007. doi: 10.1038/nature06202.

James Farquhar, John Cliff, Aubrey L Zerkle, Alexey Kamyshny, Simon W Poulton, Mark Claire, David Adams, and Brian Harms. Pathways for Neoarchean pyrite formation constrained by mass-independent sulfur isotopes. *Proceedings of the National Academy of Sciences*, 110(44): 17638–17643, 2013. ISSN 1091-6490. doi: 10.1073/pnas.1218851110.

Woodward W Fischer, David a Fike, Jena E Johnson, Timothy D Raub, Yunbin Guan, Joseph L Kirschvink, and John M Eiler. SQUID–SIMS is a useful approach to uncover primary signals in the Archean sulfur cycle. *Proceedings of the National Academy of Sciences*, 111(15):5468–5473, 2014. doi: 10.1073/pnas.1322577111.

Eugene G. Grosch and Nicola McLoughlin. Paleoarchean sulfur cycle and biogeochemical surface conditions on the early Earth, Barberton, South Africa. *Earth and Planetary Science Letters*, 377-378:142–154, 2013. doi: 10.1016/j.epsl.2013.06.035.

Qingjun Guo, Harald Strauss, Alan J. Kaufman, Stefan Schröder, Jens Gutzmer, Boswell Wing, Margaret A. Baker, Andrey Bekker, Quesheng Jin, Sang Tae Kim, and James Farquhar. Reconstructing Earth's surface oxidation across the Archean-Proterozoic transition. *Geology*, 37(5): 399–402, 2009. ISSN 00917613. doi: 10.1130/G25423A.1.

B. M. Guy, S. Ono, J. Gutzmer, A. J. Kaufman, Y. Lin, M. L. Fogel, and N. J. Beukes. A multiple sulfur and organic carbon isotope record from non-conglomeratic sedimentary rocks of the Mesoarchean Witwatersrand Supergroup, South Africa. *Precambrian Research*, 216-219: 208–231, 2012. doi: 10.1016/j.precamres.2012.06.018.

Guixing Hu, Douglas Rumble, and Pei Ling Wang. An ultraviolet laser microprobe for the in situ analysis of multisulfur isotopes and its use in measuring Archean sulfur isotope mass-independent anomalies. *Geochimica et Cosmochimica Acta*, 67(17):3101–3117, 2003. ISSN 00167037. doi: 10.1016/S0016-7037(02)00929-8.

Gareth Izon, Aubrey L. Zerkle, Iadviga Zhelezinskaia, James Farquhar, Robert J. Newton, Simon W. Poulton, Jennifer L. Eigenbrode, and Mark W. Claire. Multiple oscillations in Neoarchaean atmospheric chemistry. *Earth and Planetary Science Letters*, 431:264–273, 2015. doi: 10.1016/j.epsl.2015.09.018.

B. S. Kamber and M. J. Whitehouse. Micro-scale sulphur isotope evidence for sulphur cycling in the late Archean shallow ocean. *Geobiology*, 5(1):5–17, 2007. ISSN 14724677. doi: 10.1111/j.1472-4669.2006.00091.x.

Alan J Kaufman, David T Johnston, James Farquhar, Andrew L Masterson, Timothy W Lyons, Steve Bates, Ariel D Anbar, Gail L Arnold, Jessica Garvin, and Roger Buick. Late archean biospheric oxygenation and atmospheric evolution. *Science*, 317(5846):1900–1903, 2007.

Florian Kurzweil, Mark Claire, Christophe Thomazo, Marc Peters, Mark Hannington, and Harald Strauss. Atmospheric sulfur rearrangement 2.7 billion years ago: Evidence for oxygenic photosynthesis. *Earth and Planetary Science Letters*, 366:17–26, 2013. doi: 10.1016/j.epsl.2013.01.028.

G. Luo, S. Ono, N. J. Beukes, D. T. Wang, S. Xie, and R. E. Summons. Rapid oxygenation of Earths atmosphere 2.33 billion years ago. *Science Advances*, 2(5):e1600134, 2016. doi: 10.1126/sciadv.1600134.

S. J. Mojzsis, C. D. Coath, J. P. Greenwood, K. D. McKeegan, and T. M. Harrison. Mass-independent isotope effects in Archean (2.5 to 3.8 Ga) sedimentary sulfides determined by ion microprobe analysis. *Geochimica et Cosmochimica Acta*, 67(9):1635–1658, 2003. ISSN 00167037. doi: 10.1016/S0016-7037(00)00059-0.

Alice Montinaro, Harald Strauss, Paul R D Mason, Desiree Roerdink, Carsten M??nker, Ulrich Schwarz-Schampera, Nicholas T. Arndt, James Farquhar, Nicolas J. Beukes, Jens Gutzmer, and Marc Peters. Paleoarchean sulfur cycling: Multiple sulfur isotope constraints from the Barberton Greenstone Belt, South Africa. *Precambrian Research*, 267:311–322, 2015.

Hiroshi Ohmoto, Yumiko Watanabe, Hiroaki Ikemi, Simon R. Poulson, and Bruce E. Taylor. Sulphur isotope evidence for an oxic Archaean atmosphere. *Nature*, 442(7105):908–911, 2006. doi: 10.1038/nature05044.

Shuhei Ono, Jennifer L. Eigenbrode, Alexander A. Pavlov, Pushker Kharecha, Douglas Rumble, James F. Kasting, and Katherine H. Freeman. New insights into Archean sulfur cycle from mass-independent sulfur isotope records from the Hamersley Basin, Australia. *Earth and Planetary Science Letters*, 213(1-2):15–30, 2003. ISSN 0012821X. doi: 10.1016/S0012-821X(03)00295-4.

Shuhei Ono, Boswell Wing, Douglas Rumble, and James Farquhar. High precision analysis of all four stable isotopes of sulfur (^{32}S, ^{33}S, ^{34}S and ^{36}S) at nanomole levels using a laser fluorination isotope-ratio-monitoring gas chromatographymass spectrometry. *Chemical Geology*, 225(1-2): 30–39, 1 2006. doi: 10.1016/j.chemgeo.2005.08.005.

Shuhei Ono, Alan J. Kaufman, James Farquhar, Dawn Y. Sumner, and Nicolas J. Beukes. Lithofacies control on multiple-sulfur isotope records and Neoarchean sulfur cycles. *Precambrian Research*, 169(1-4):58–67, 2009a. ISSN 03019268. doi: 10.1016/j.precamres.2008.10.013.

Shuhei Ono, Nicolas J. Beukes, and Douglas Rumble. Origin of two distinct multiple-sulfur isotope compositions of pyrite in the 2.5 Ga Klein Naute Formation, Griqualand West Basin, South Africa. *Precambrian Research*, 169(1-4):48–57, 2009b. ISSN 03019268. doi: 10.1016/j.precamres.2008.10.012.

Dominic Papineau, S. J. Mojzsis, C. D. Coath, J. A. Karhu, and K. D. McKeegan. Multiple sulfur isotopes of sulfides from sediments in the aftermath of Paleoproterozoic glaciations. *Geochimica et Cosmochimica Acta*, 69(21):5033–5060, 2005. ISSN 00167037. doi: 10.1016/j.gca.2005.07.005.

D. Papineau and S. J. Mojzsis. Mass-independent fractionation of sulfur isotopes in sulfides from the pre-3770 Ma Isua Supracrustal Belt, west Greenland. *Geobiology*, 4(4):227–238, 2006. ISSN 14724677. doi: 10.1111/j.1472-4669.2006.00083.x.

Michaela A. Partridge, Suzanne D. Golding, Kim A. Baublys, and Elisa Young. Pyrite paragenesis and multiple sulfur isotope distribution in late Archean and early Paleoproterozoic Hamersley Basin sediments. *Earth and Planetary Science Letters*, 272(1-2):41–49, 2008. ISSN 0012821X. doi: 10.1016/j.epsl.2008.03.051.

Pascal Philippot, Mark van Zuilen, and Claire Rollion-Bard. Variations in atmospheric sulphur chemistry on early Earth linked to volcanic activity. *Nature Geoscience*, 5(9):668–674, 2012. doi: 10.1038/ngeo1534.

Desiree L. Roerdink, Paul R D Mason, Martin J. Whitehouse, and Thomas Reimer. High-resolution quadruple sulfur isotope analyses of 3.2Ga pyrite from the Barberton Greenstone Belt in South Africa reveal distinct environmental controls on sulfide isotopic arrays. *Geochimica et Cosmochimica Acta*, 117:203–215, 2013. doi: 10.1016/j.gca.2013.04.027.

Emilie Thomassot, Jonathan ONeil, Don Francis, Pierre Cartigny, and Boswell A. Wing. Atmospheric record in the Hadean Eon from multiple sulfur isotope measurements in Nuvvuagittuq Greenstone Belt (Nunavik, Quebec). *Proceedings of the National Academy of Sciences*, 112(3): 707–712, 2015. doi: 10.1073/pnas.1419681112.

Christophe Thomazo, M. Ader, J. Farquhar, and P. Philippot. Methanotrophs regulated atmospheric sulfur isotope anomalies during the Mesoarchean (Tumbiana Formation, Western Australia). *Earth and Planetary Science Letters*, 279(1-2):65–75, 2009. doi: 10.1016/j.epsl.2008.12.036.

Yuichiro Ueno, Shuhei Ono, Douglas Rumble, and Shigenori Maruyama. Quadruple sulfur isotope analysis of ca. 3.5 Ga Dresser Formation: New evidence for microbial sulfate reduction in the early Archean. *Geochimica et Cosmochimica Acta*, 72(23):5675–5691, 2008. doi: 10.1016/j.gca.2008.08.026.

Martin J. Whitehouse, Balz S. Kamber, Christopher M. Fedo, and Aivo Lepland. Integrated Pb- and S-isotope investigation of sulphide minerals from the early Archaean of southwest Greenland. *Chemical Geology*, 222(1-2):112–131, 2005. ISSN 00092541. doi: 10.1016/j.chemgeo.2005.06.004.

Aubrey L. Zerkle, Mark W. Claire, Shawn D. Domagal-Goldman, James Farquhar, and Simon W. Poulton. A bistable organic-rich atmosphere on the Neoarchaean Earth. *Nature Geoscience*, 5 (5):359–363, 2012. doi: 10.1038/ngeo1425.

I. Zhelezinskaia, A. J. Kaufman, J. Farquhar, and J. Cliff. Large sulfur isotope fractionations associated with Neoarchean microbial sulfate reduction. *Science*, 346(6210):742–744, 2014. doi: 10.1126/science.1256211.

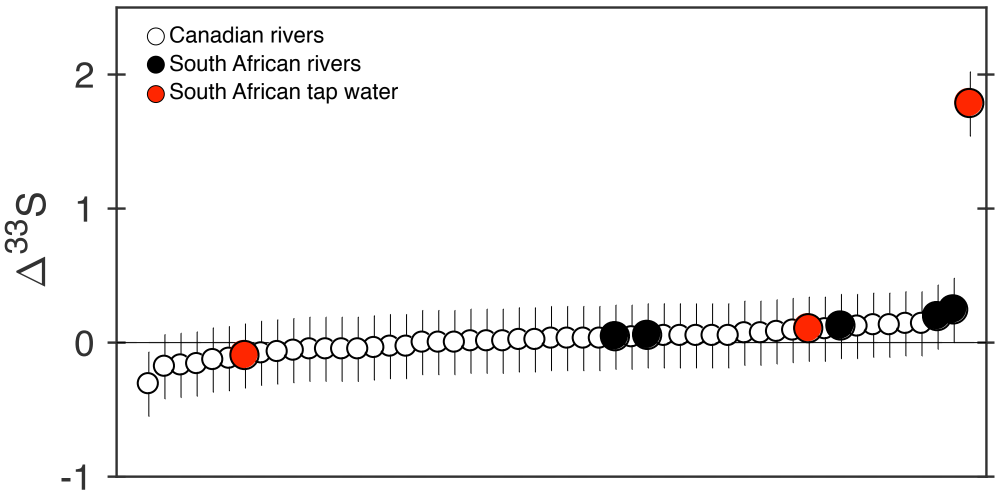

Figure S1: Sulfur isotopic ratios of Canadian and South African samples. A majority of dissolved sulfate sourced from the weathering of Archean rocks has a $\Delta^{33}S \approx 0$ ‰. While one groundwater sample from a carbonate aquifer has a higher value, we hypothesized that this sample averages over a small volume of rock and thus not representative of the bulk crust. Error bars represent one standard deviation of the analytical uncertainty.

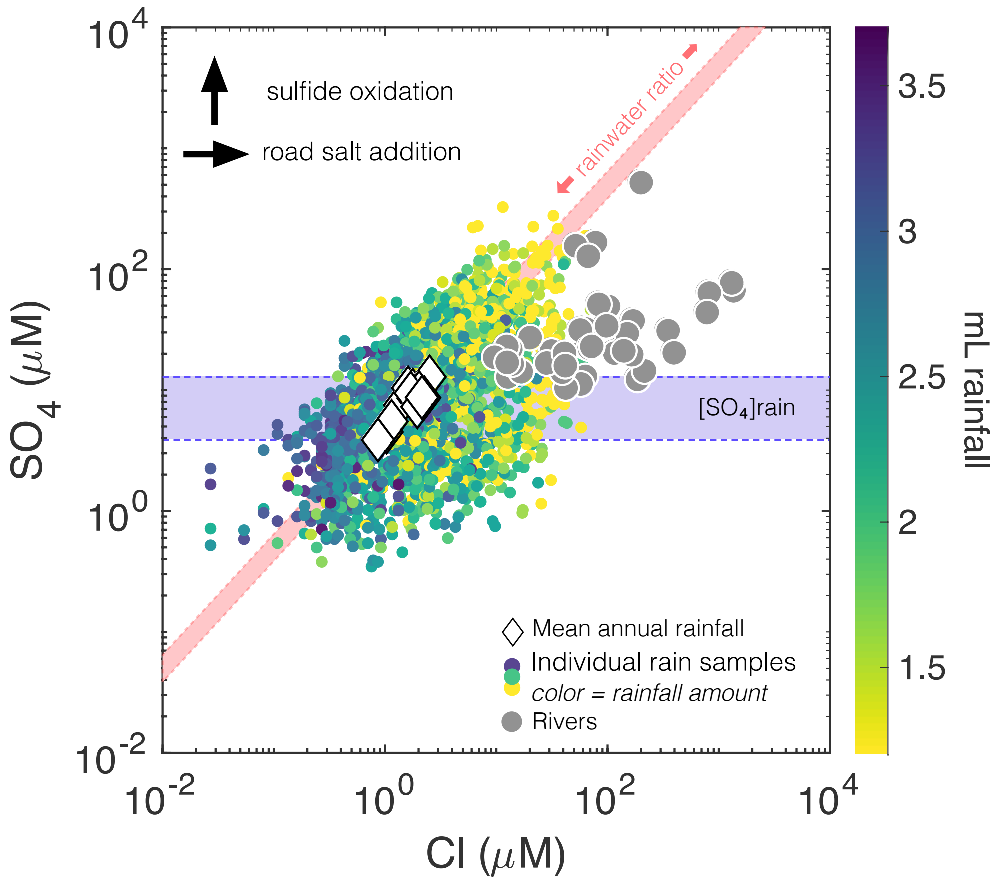

Figure S2: The chloride and sulfate concentrations of daily rainwater samples (colored points) compared with precipitation-weighted mean annual rainfall (diamonds) and river waters (gray circles) in the Great Lakes region of Canada. The daily rainfall samples are color-coded based on the volume of precipitation that fell during the collection day. We assumed that the sulfate concentration of mean annual rainfall represents the minimum concentration of river water and that excess sulfate in river water derives from rock weathering.

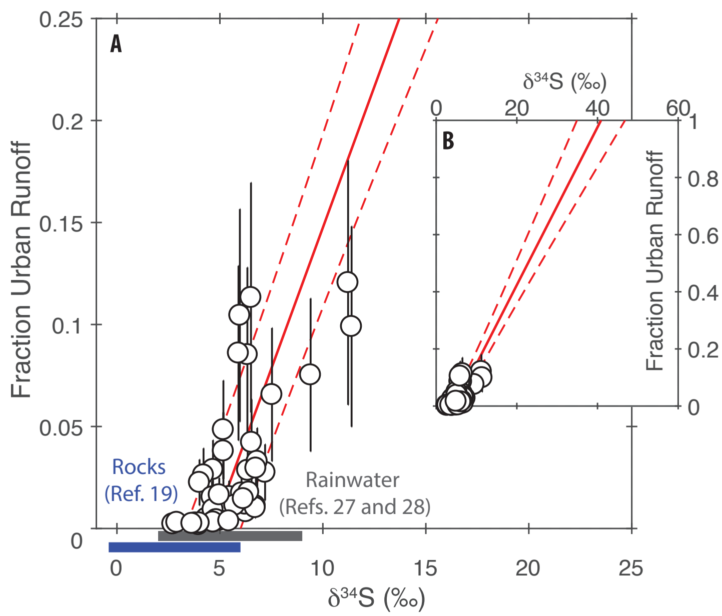

Figure S3: δ^{34}S of Canadian Rivers. (a) Measured δ^{34}S values of riverine sulfate and the inferred proportion of sulfate sourced from urban runoff (mean and one standard deviation). The red trend line refers to a linear regression using the mean proportions of urban runoff sourced sulfate. (b) Same as in (a) but showing the predicted δ^{34}S of urban runoff based on the liner regression. The dash lines show the 68% confidence interval.

Table S1: Sulfide Mineral $\Delta^{33}S$ Compilation

First Author	Year	Citation
Cates	2006	(Cates and Mojzsis, 2006)
Farquhar	2000,2007,2013	(Farquhar et al., 2000, 2007, 2013)
Fischer	2014	(Fischer et al., 2014)
Grosch	2013	(Grosch and McLoughlin, 2013)
Guo	2009	(Guo et al., 2009)
Guy	2012	(Guy et al., 2012)
Hu	2003	(Hu et al., 2003)
Izon	2015	(Izon et al., 2015)
Kamber	2007	(Kamber and Whitehouse, 2007)
Kaufman	2007	(Kaufman et al., 2007)
Kurzweil	2013	(Kurzweil et al., 2013)
Luo	2016	(Luo et al., 2016)
Mojzis	2003	(Mojzsis et al., 2003)
Montinaro	2015	(Montinaro et al., 2015)
Ohmoto	2006	(Ohmoto et al., 2006)
Ono	2003,2006,2009a,2009b	(Ono et al., 2003, 2006, 2009a,b)
Papineau	2005,2008	(Papineau et al., 2005; Papineau and Mojzsis, 2006)
Partridge	2009	(Partridge et al., 2008)
Philippot	2012	(Philippot et al., 2012)
Roerdink	2013	(Roerdink et al., 2013)
Thomassot	2015	(Thomassot et al., 2015)
Thomazo	2009	(Thomazo et al., 2009)
Ueno	2008	(Ueno et al., 2008)
Whitehouse	2005,2008	(Whitehouse et al., 2005)
Zerkle	2012	(Zerkle et al., 2012)
Zhelezinskaia	2014	(Zhelezinskaia et al., 2014)

Table S2: Superior Craton Data

Name	Area (km^2)	Latitude	Longitude	Cl (μM)	SO_4 (μM)	δ^{34}S (‰)	Δ^{33}S (‰)	% Archean
Kaministiquia River	7705.0	48.340	-89.333	358.7	30.3	7.5	-0.2	91
Lakehead	150.1	48.422	-89.265	1402.9	64.8	11.2	0.0	88
Madeline	43.2	48.451	-89.235	1339	75.5	11.4	0.0	89
Current River	603.0	48.469	-89.199	144.2	27.8	6.4	0.1	98
Mackenzie River	358.4	48.535	-88.941	64.9	22.5	5.5	0.1	86
Wolf River	603.2	48.822	-88.539	32.1	20.6	6.3	0.1	34
Black Sturgeon River	2709.4	48.905	-88.376	842.3	62.1	9.4	0.0	30
Helen Lake	25589.4	49.037	-88.250	406.8	19.9	6.5	0.0	57
Gorge Creek	39.6	49.302	-88.099	13	12.6	4.4	0.0	0
Blackwater River	484.6	49.609	-87.957	190.6	12	6.3	0.0	100
Longlac	1690.3	49.784	-86.539	64.7	12.7	7.2	-0.1	100
Skunk River	176.6	49.761	-84.484	65	31.4	6.7	-0.1	100
Mattawishkwia River	1034.3	49.686	-83.633	220.2	14.1	5.9	0.0	100
Missinaibi River	10363.6	49.615	-83.265	17.1	13.9	5.2	0.0	100
Opasatika River	1337.2	49.525	-82.841	59.1	11	4.7	0.0	100
Kapuskasing River	3372.8	49.391	-82.445	173.9	36.5	4.2	0.0	100
Poplar Rapids River	126.1	49.289	-81.784	43.3	10.2	4.0	-0.1	100
Mattagami River (1)	9041.5	49.275	-81.636	104.6	48	6.2	0.0	98
Hunta	598.0	49.058	-81.244	40	13.8	4.6	0.1	100
Fredrick House River	3300.6	49.059	-81.138	79.9	162.2	3.8	-0.1	97
Driftwood River	531.7	48.634	-80.682	158.9	20.7	6.5	0.1	100
Night Hawk Lake	2327.7	48.549	-80.975	52.9	153	4.0	-0.1	96
Mattagami River (2)	6335.1	48.476	-81.351	58.1	30.7	6.7	0.1	98
Opishing River	87.9	48.239	-81.848	29.1	16.4	5.3	-0.2	100
Groundhog River	3680.5	48.203	-82.173	69.9	21.8	6.1	-0.1	100
N. Chapleau Lake	139.9	47.845	-83.407	118.9	19.8	6.8	0.1	100
S. Chapleau Lake	296.1	47.842	-83.396	154	28.6	6.8	0.0	100
Chapleau Hotel	NaN	47.842	-83.398	205.6	508.4	2.7	0.1	NaN
Grazing River	123.1	47.855	-83.795	73.8	22.5	6.4	0.1	100
Jackpine River (1)	1659.4	47.945	-84.153	42	19.7	5.7	-0.1	100
Michipicoten River	4227.7	47.944	-84.529	20.6	26.6	5.0	-0.2	100
Magpie River	1958.6	47.986	-84.798	85.6	50.1	4.7	-0.3	100
Depew River	245.7	48.536	-85.172	169	19.2	5.2	0.0	100
White River	1027.2	48.588	-85.307	143.2	20.7	5.2	-0.1	100
Pic tributary	2168.7	48.688	-86.213	68.8	125.2	2.9	0.1	100
Pic River	3702.8	48.770	-86.297	13.2	19.8	4.7	0.1	100
Little Pic River	2076.8	48.801	-86.631	14.2	16.1	4.8	0.0	94
Steel River tributary	7.1	48.775	-86.882	806	42.8	6.0	0.0	100
Steel River	1175.3	48.777	-86.884	13.8	21.3	4.7	0.1	100
Pays Plat River	427.6	48.882	-87.560	12.7	22.5	4.0	0.1	99
Cypress River	117.7	48.934	-87.865	9.9	18.3	3.6	0.1	99
Jackpine River (2)	275.0	48.977	-87.998	12.8	16.6	5.4	0.1	99
Jackfish River	463.4	49.008	-88.078	42.7	15.6	6.1	0.0	85
Best Western Hotel	NaN	48.381	-89.299	100.5	33.3	5.0	-0.1	NaN

Table S3: Kaapvaal Craton Data

Name	Latitude	Longitude	δ^{34}S (‰)	Δ^{33}S (‰)
Maroela Guest House	-24.595	27.406	6.1	-0.1
Mfolozi River	-28.238	-31.176	6.8	0.0
Vryheid B&B	-27.769	30.792	9.2	0.1
Harts River (1)	-26.383	25.910	10.4	0.2
Rus 'n Bietjie	-28.163	23.558	7.1	1.8
Harts River (2)	-27.571	24.743	14.3	0.0
Elands River	-25.334	27.292	6.6	0.1
Crocodile River	-24.653	27.379	7.5	0.2